

This is the accepted manuscript made available via CHORUS. The article has been published as:

Magnetic field dependence of the Schottky anomaly in filled skutterudites $\text{Pr}_{1-x}\text{Eu}_x\text{Pt}_4\text{Ge}_{12}$

R. B. Adhikari, P. Shen, D. L. Kunwar, I. Jeon, M. B. Maple, M. Dzero, and C. C. Almasan

Phys. Rev. B **100**, 174509 — Published 8 November 2019

DOI: [10.1103/PhysRevB.100.174509](https://doi.org/10.1103/PhysRevB.100.174509)

Magnetic field dependence of the Schottky anomaly in filled skutterudites $\text{Pr}_{1-x}\text{Eu}_x\text{Pt}_4\text{Ge}_{12}$

R. B. Adhikari,¹ P. Shen,¹ D. L. Kunwar,¹ I. Jeon,^{2,3} M. B. Maple,^{2,3,4} M. Dzero,¹ and C. C. Almasan¹

¹*Department of Physics, Kent State University, Kent, Ohio, 44242, USA*

²*Center for Advanced Nanoscience, University of California, San Diego, La Jolla, California 92093, USA*

³*Materials Science and Engineering Program, University of California, San Diego, La Jolla, California 92093, USA*

⁴*Department of Physics, University of California at San Diego, La Jolla, CA 92093, USA*

(Dated: October 17, 2019)

By performing a series of thermodynamic measurements in an applied magnetic field H_{ext} , we investigated the effects of Eu substitution on the Pr sites in filled skutterudite compound $\text{Pr}_{1-x}\text{Eu}_x\text{Pt}_4\text{Ge}_{12}$ ($0 \leq x \leq 1$). A heat capacity Schottky anomaly is present over the whole doping range. For the samples with $x > 0.5$, the temperature of the maximum T_{max} shifts to lower temperature with increasing H_{ext} . We argue that this behavior reflects the antiferromagnetic (AFM) ordering of the Eu moments, as the AFM transition is suppressed by H_{ext} . The Schottky anomaly in the samples with $x \leq 0.5$ shift to higher temperatures with increasing magnetic field, signaling the presence of an internal magnetic field due to short-range AFM correlations induced by magnetic moments of neighboring Eu sites. In low H_{ext} , the Schottky gaps show a non-linear relationship with H_{ext} as the magnetic moments become weakly magnetized. In high H_{ext} , the magnetic moments of Eu sites become completely aligned with H_{ext} . Thus, increasing H_{ext} does not further increase the magnetization, hence the Schottky gaps increase linearly with H_{ext} .

PACS numbers: 71.10.Ay, 74.25.F-, 74.62.Bf, 75.20.Hr

INTRODUCTION

A competition and/or possible coexistence between unconventional superconductivity and various - possibly nontrivial - magnetic ground states in filled skutterudite compounds with the chemical formula $\text{MPt}_4\text{Ge}_{12}$ (where M denotes alkaline earth, lanthanide, or actinide) provides a major motivation for further exploring the physics of these compounds. As a result, these materials have attained recently a renewed experimental and theoretical interest.

$\text{PrPt}_4\text{Ge}_{12}$ has a surprisingly high critical temperature of $T_c \simeq 7.9$ K among superconducting members of Pr-based skutterudites and a moderately low Sommerfeld coefficient of $\gamma \sim 60$ mJ/(mol·K²), corresponding to a medium enhancement of the conduction electron effective mass [1]. It is important to keep in mind that $\text{PrPt}_4\text{Ge}_{12}$ is also a multiband superconductor [2–4] with two Fermi surfaces, having one nodal and one nodeless gap, indicating the unconventional nature of superconductivity (SC) [5]. Specifically, its multiband nature may be the main reason why superconductivity remains fairly robust with respect to introducing disorder by chemical substitutions [5]. Another feature pointing towards the unconventional symmetry of superconducting pairing in these compounds is the observation of the time-reversal symmetry breaking in the superconducting state of $\text{PrPt}_4\text{Ge}_{12}$ [6] and $\text{PrOs}_4\text{Sb}_{12}$ [7].

The ions Eu^{2+} (or Gd^{3+}) have large total angular momentum $J = S = 7/2$ and, hence, the compounds containing such ions exhibit large magnetic moments. Consequently, these compounds typically exhibit magnetic

ordering. Some of the filled skutterudite systems with Eu^{2+} electronic configuration, such as $\text{EuFe}_4\text{Sb}_{12}$ and $\text{EuFe}_4\text{As}_{12}$, indeed, show magnetic ordering at Curie temperature $T_C \sim 88$ K and ~ 152 K [8, 9], respectively, where the higher T_C has been attributed to the existence of an additional, albeit small, magnetic moment $\sim 0.21\mu_B$ per Fe atom [10], i.e. $0.83\mu_B$ for $\text{Fe}_4\text{Sb}_{12}$. The $\text{MFe}_4\text{Sb}_{12}$ compounds with itinerant FM order of the $\text{Fe}_4\text{Sb}_{12}$ cage generally have $T_C \sim 80$ K [11]. Furthermore, $\text{EuPt}_4\text{Ge}_{12}$ displays antiferromagnetism (AFM) with a Néel critical temperature $T_N \sim 1.78$ K, an effective magnetic moment of $\mu_{\text{eff}} = 7.4\mu_B$, and a Curie-Weiss temperature $\Theta_{CW} \sim -11$ K [12, 13]. The lower magnetic ordering temperature for $\text{EuPt}_4\text{Ge}_{12}$ may be due to the absence of a magnetic moment on Pt in the Pt-Ge cage, causing a decrease in the exchange coupling determined by the Ruderman-Kittel-Kasuya-Yosida (RKKY) interaction between the Eu^{2+} localized magnetic moments and the conduction-electron spins [10, 13]. This scenario is supported by lower ordering temperatures in $\text{EuRu}_4\text{Sb}_{12}$ and $\text{EuOs}_4\text{Sb}_{12}$ ferromagnets with $T_C = 4$ and 9 K, respectively, that lack magnetic moments in Ru-Sb and Os-Sb cages [8].

Heat capacity measurements of Eu^{2+} or Gd^{3+} containing samples, such as $(\text{Sn}_{1-x}\text{Eu}_x)\text{Mo}_6\text{S}_8$ [14], $\text{Ba}_{8-x}\text{Eu}_x\text{Ge}_{43}\square_3$ [15], and $\text{RuSr}_2(\text{Gd}_{1.5}\text{Ce}_{0.5})\text{Cu}_2\text{O}_{10-\delta}$ [16], have been found to exhibit upturn in C_e/T upon lowering the temperature. This upturn is due to a Schottky anomaly resulting from the splitting of the ground state octet of Eu/Gd by the internal molecular and externally applied magnetic field. The upturns in C_e/T vs T data of some skutterudites containing Pr such as $\text{PrOs}_4\text{Sb}_{12}$ [17], $\text{Pr}(\text{Os}_{1-x}\text{Ru}_x)_4\text{Sb}_{12}$ [18] and $\text{PrRu}_4\text{Sb}_{12}$

[19] have been attributed to crystalline electric field (CEF) splitting of the ground state of Pr^{3+} ions [20], while the upturns below 0.5 K in zero field in $\text{PrPt}_4\text{Ge}_{12}$ [1, 5] and $\text{PrOs}_4\text{Sb}_{12}$ [21] have been attributed to the high temperature tail of the nuclear Schottky anomaly of ^{141}Pr nuclei with nuclear spin $I = 5/2$.

All the results discussed above show that, at least in principle, it should be possible to probe the signatures of magnetic correlations by analyzing the Schottky contribution to the heat capacity. We performed low-temperature specific heat measurements on samples of $\text{Pr}_{1-x}\text{Eu}_x\text{Pt}_4\text{Ge}_{12}$ in magnetic field. Our detailed and systematic analysis indicates that the upturns in the heat capacity are caused by the splitting of the octet degenerate states of Eu^{2+} due to the internal magnetic field produced by the net magnetic moment \mathbf{m} present as a result of short-range antiferromagnetic correlations between the nearest-neighbor Eu ions [22]. We have also systematically analyzed the effect of applied magnetic field on the temperature T_{max} of the maximum of the Schottky anomaly. Our analysis shows that T_{max} increases linearly with increasing magnetic field in the samples with high Eu content and in the high magnetic field region. For the low Eu-substituted samples and in the low magnetic field region, T_{max} shows a super-linear magnetic field dependence since increasing applied magnetic field continuously rotates the direction of the net moment, resulting in a decrease of the S_z antiparallel to the applied field.

EXPERIMENTAL DETAILS

$\text{Pr}_{1-x}\text{Eu}_x\text{Pt}_4\text{Ge}_{12}$ samples were synthesized by arc-melting and annealing from high purity Pr ignots, Eu ignots, Pt sponge, and Ge pieces according to the procedure described in detail in Ref. [23]. The crystal structure was determined through X-ray powder diffraction using a Bruker D8 Discover X-ray diffractometer with $\text{Cu-K}\alpha$ radiation, and the XRD patterns were analysed through Rietveld refinement [24]. A detailed sample characterization of the series of these polycrystalline samples through X-ray diffraction, electrical resistivity, and magnetic susceptibility, as described elsewhere [25], shows the purity of the samples used in this study.

One surface of each sample was polished with sand paper to improve the contact between the sample and the specific heat platform. We performed a series of specific heat measurements on the polycrystalline samples of $\text{Pr}_{1-x}\text{Eu}_x\text{Pt}_4\text{Ge}_{12}$ with $x = 0, 0.05, 0.10, 0.15, 0.20, 0.30, 0.38, 0.50, 0.70, 0.80, 0.90$, and 1.00 in applied magnetic field H_{ext} up to 14 T over the temperature T range $0.50 \text{ K} \leq T \leq 10 \text{ K}$. The specific heat measurements were performed via a standard thermal relaxation technique using the He-3 option of a Quantum Design Physical Property Measurement System (PPMS).

RESULTS AND DISCUSSION

The measured specific heat in the normal state $C(T) = \gamma_n T + BT^3$ is the sum of electronic $C_e \equiv \gamma_n T$ (γ_n is the normal-state Sommerfeld coefficient) and phonon $C_{ph} \equiv BT^3$ contributions; hence, we did a least-squares fit of C/T vs T^2 data in the normal state ($T_c < T \leq 15 \text{ K}$) for different Eu concentrations, as described and shown in Fig. 1 of ref. [22], in order to determine γ_n and B . We then subtracted the phonon contribution to the specific heat for all the measured samples of $\text{Pr}_{1-x}\text{Eu}_x\text{Pt}_4\text{Ge}_{12}$. We subtracted the same phonon contribution from the specific heat data measured in an applied magnetic field H_{ext} , thus assuming that the phonon contribution is field independent.

Figures 1(a), 1(b), and 1(c) display the specific heat vs T data for the $x = 0.05, 0.50$, and 0.80 , respectively, samples measured in different applied magnetic fields H_{ext} . These figures reveal upturns present in the specific heat data below 2 K. For the samples with $x \leq 0.15$, the specific heat shows an upturn without reaching a maximum [Fig. 1(a)], whereas the samples with larger x values show a clear maximum present in the low-temperature region [Figs. 1(b) and 1(c)].

With increasing applied magnetic field H_{ext} , the samples with $0.05 \leq x \leq 0.15$ begin to show a distinct maximum [Fig. 1(a)], while the samples with $x \leq 0.5$ show that the maximum becomes broader, shifts to higher temperatures, and decreases in amplitude [Fig. 1(b)]. The Schottky anomaly for the $0.7 \leq x \leq 1$ samples in low applied magnetic field reveals a long-range AFM transition at T_N , see inset Fig. 1(c), that, as expected, shift to lower temperatures with increasing H_{ext} . Nevertheless, once the AFM transition is suppressed below the lowest measured temperature of 0.5 K, the maximum of the Schottky anomaly shifts to higher temperatures with further increase in H_{ext} [Fig. 1(c)], as also observed in the $x < 0.5$ samples [Figs. 1(a) and 1(b)].

We note that a superconducting transition at a temperature T_c is clearly seen in the heat capacity of the samples with $0 \leq x \leq 0.3$ [22]. The superconducting jump becomes broader and T_c shifts to lower temperatures, as expected, with increasing H_{ext} and increasing Eu concentration [22]. The samples with $0.3 < x \leq 0.5$ show a superconducting transition only in resistivity measurements [25], while the samples with $x > 0.5$ do not display a superconducting transition for temperatures down to $T = 0.5 \text{ K}$.

We have attributed the Schottky anomaly present in the heat capacity data of the $x \leq 0.5$ samples to the splitting of the degenerate $^8S_{7/2}$ ground state of Eu^{2+} into eight equally-spaced energy levels, as shown schematically in Fig. 2(a), by both the external H_{ext} and internal H_{int} magnetic fields. The effective field has, hence, two contributions: $\mathbf{H}_{eff} \equiv \mathbf{H}_{int} + \mathbf{H}_{ext}$. The internal field H_{int}

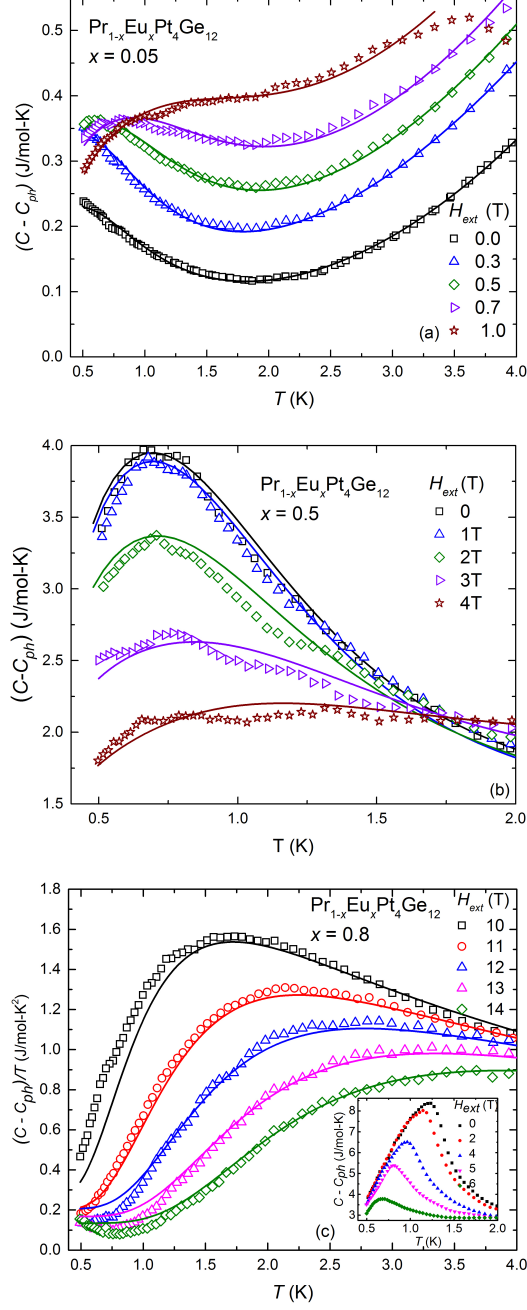


FIG. 1: (Color online) Specific heat $C - C_{ph}$ vs temperature T of $\text{Pr}_{1-x}\text{Eu}_x\text{Pt}_4\text{Ge}_{12}$ measured in different magnetic fields H for the (a) $x = 0.05$, (b) $x = 0.50$, and (c) $x = 0.80$ samples. The solid curves are fits of the data using the sum of Schottky and superconducting contributions for (a) and (b), and Schottky and normal-state contributions for (c), as described in the text.

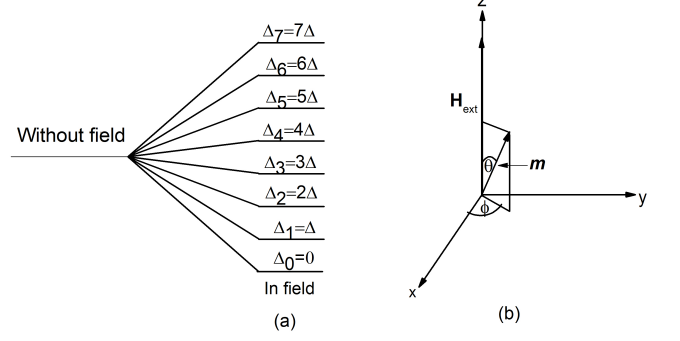


FIG. 2: (Color online) (a) Splitting of the ground state $^8S_{7/2}$ of Eu into 8 equally-spaced energy levels by both internal and external magnetic fields. (b) Schematic representation of the net magnetic moment \mathbf{m} and external magnetic field pointing in different directions.

is due to the net magnetic moment \mathbf{m} present as a result of short-range antiferromagnetic correlations between the nearest-neighbor Eu ions [22]. These short-range antiferromagnetic correlations co-exist with superconductivity in these lower Eu substituted samples (see Fig. 7 of Ref. [22]). We note that one may expect short-range antiferromagnetic correlations between the Eu ions to be present in the alloys $\text{Pr}_{1-x}\text{Eu}_x\text{Pt}_4\text{Ge}_{12}$ since $\text{EuPt}_4\text{Ge}_{12}$ orders antiferromagnetically.

The Schottky heat capacity anomaly for an eight-energy-levels system with the degeneracy fully lifted by magnetic field is given by [26]

$$C_{\text{Sch}} = r(x) \frac{R}{T^2} \left[\frac{f_2(T)}{f_0(T)} - \frac{f_1^2(T)}{f_0^2(T)} \right], \quad (1)$$

$$f_m(T) = \sum_{j=0}^7 \Delta_j^m \exp \left(-\frac{\Delta_j}{k_B T} \right), \quad m = 0, 1, 2$$

where $r(x)$ is one of the fitting parameters and it turns out that it represents the concentration of Eu ions [22], $R = 8.31$ J/mol-K is the universal gas constant, $\Delta_j = j \cdot \Delta$ is the energy gap between the lowest energy level ($j = 0$) and the j^{th} energy level, $\Delta \equiv g\mu_B H_{\text{eff}}/k_B$, $g = 2$ ($L = 0$), and μ_B is the Bohr magneton. Hence, the value of the Schottky gap Δ fully depends on H_{eff} .

As just mentioned, the lower Eu-doped samples ($0.05 \leq x \leq 0.5$) have two contributions to the heat capacity in the low field and low temperature ($0.5 \leq T < T_c$) region: Schottky and superconducting contributions. Specifically, for the samples with Eu concentrations in the range $0.05 \leq x \leq 0.15$, the superconducting contribution is best described by $(C - C_{ph}) \propto T^2$, i.e., line

nodes in the superconducting gap, while for $0.2 \leq x \leq 0.5$ by $(C - C_{ph}) \propto \exp^{-\delta/T}$, i.e., by an isotropic gap; this is expected since the nodal gap is quickly suppressed by scattering on lattice imperfections. In the high field region where $T_c < 0.5$ K or for the $x \geq 0.7$ samples, the total specific heat is the sum of Schottky and normal-state electronic ($\gamma_n T$) contributions. Least-squares fits of the data are shown by the solid curves in Figs. 1(a) through 1(c). The fitted curves are in excellent agreement with the measured specific heat data.

The effect of Eu substitution on unconventional superconductivity has been previously studied and it has been found that the Eu magnetic moment is unfavorable to superconductivity [27, 28], while in some cases the magnetic ordering of Eu moments co-exists with superconductivity [29, 30] and superconductivity remains surprisingly robust in the presence of Eu local moments[22]. For example, in our earlier work [22], we have shown that superconductivity is fully suppressed when Eu concentration reaches about 60 %, which is far beyond the impurity limit. Our present work helps to understand such a robustness: indeed, if antiferromagnetically ordered clusters of Eu ions have a typical size smaller than the coherence length, their destructive effect of superconductivity is expected to be diminished compared to the opposite limit when the coherence length were smaller than the typical size of a cluster. Qualitative support for this argument also comes from the observation that superconductivity in the Pr-based systems most likely belongs to the weak coupling limit, so that the coherence length is of the order of 10^{-6} m.

The values of the Schottky gaps obtained from these fits are plotted as a function of applied magnetic field H_{ext} for various Eu substitutions in Figs. 3 and 4. We note that the Schottky gap Δ for a system with eight equally-spaced energy levels and the degeneracy fully lifted is also given by the temperature corresponding to the maximum of the Schottky anomaly, i.e., $\Delta \approx T_{\text{max}}$. The values of Δ obtained from fits (as discussed above) and from T_{max} for the samples for which the maximum of the Schottky anomaly is clearly observed are in excellent agreement. Hence, some Δ values shown in these figures for some x and/or H_{ext} values were also extracted from T_{max} . Notice that the Schottky gaps are super-linear in H_{ext} for small values of H_{ext} and increase linearly with H_{ext} with a doping-independent slope for large values of H_{ext} .

We gained an understanding of the physics that governs the behavior of these materials in the presence of an applied magnetic field as follows. Taking $\mathbf{H}_{\text{ext}} = H_{\text{ext}} \hat{z}$, and writing $\mathbf{H}_{\text{int}} = H_x \hat{x} + H_y \hat{y} + H_z \hat{z}$, gives $\langle \mathbf{H}_{\text{eff}}^2 \rangle = \langle H_x^2 + H_y^2 + (H_{\text{ext}} + H_z)^2 \rangle$. To obtain a function that describes the effective field at intermediate field values, we treat the magnetic degrees of freedom as classical, freely-rotating magnetic moments \mathbf{m} . The energy of the magnetic moment is $E = -m H_{\text{ext}} \cos \theta$, where θ is the angle

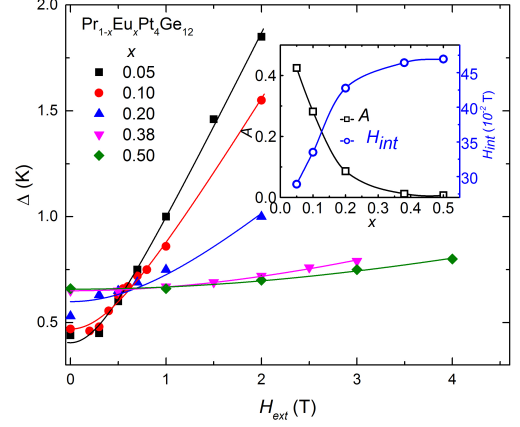


FIG. 3: (Color online) Plots of the Schottky gap Δ vs H_{ext} , for relatively small applied magnetic fields. The solid curves are fits of the data as discussed in the text. Inset: Fitting parameters A (left vertical axis) and H_{int} (right vertical axis) plotted as a function of Eu-substitution x .

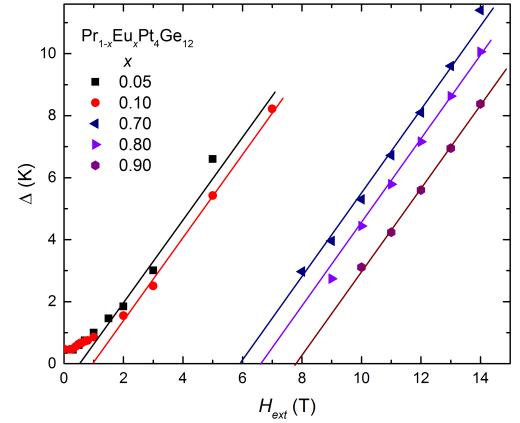


FIG. 4: (Color online) Plots of Δ vs H data for high applied magnetic fields. The straight lines are guides to the eye and show that all the Δ vs H plots have same slope of (1.4 ± 0.04) K/T.

between \mathbf{H}_{ext} and \mathbf{m} [see Fig. 2(b)] with $\mathbf{H}_{\text{int}} = -\mathbf{m}$. The partition function is then:

$$Z = \int_0^{2\pi} d\phi \int_0^\pi d\theta \sin \theta e^{\beta m H_{\text{ext}} \cos \theta} = 4\pi \frac{\sinh \beta m H_{\text{ext}}}{\beta m H_{\text{ext}}} \quad (2)$$

The expectation value of $\mathbf{H}_{\text{eff}}^2$ is

$$\begin{aligned} \langle \mathbf{H}_{\text{eff}}^2 \rangle &= \frac{1}{Z} \int_0^{2\pi} d\phi \int_0^\pi d\theta \sin \theta e^{\beta m H_{\text{ext}} \cos \theta} \times \\ &\quad [(H_{\text{ext}} - H_{\text{int}}(x) \cos \theta)^2 + (H_{\text{int}}(x) \sin \theta)^2] \quad (3) \\ &= H_{\text{ext}}^2 + H_{\text{int}}^2(x) - 2H_{\text{ext}}H_{\text{int}}(x)L(\beta m H_{\text{ext}}), \end{aligned}$$

where the Langevin function is $L(\beta m H_{\text{ext}}) = \coth(\beta m H_{\text{ext}}) - 1/(\beta m H_{\text{ext}})$ and $H_{\text{int}}(x)$ is proportional to the concentration of Eu atoms. In the limit $H_{\text{ext}} \rightarrow 0$, we find $\langle \mathbf{H}_{\text{eff}}^2 \rangle \approx H_{\text{int}}^2(x)$, so for $\beta m H_{\text{ext}} \ll 1$ it follows that $L(\beta m H_{\text{ext}}) \approx (\beta m H_{\text{ext}})/3$ and $\langle \mathbf{H}_{\text{eff}}^2 \rangle = H_{\text{ext}}^2 - 2/3 H_{\text{ext}}^2 H_{\text{int}}(x) \beta m + H_{\text{int}}^2(x)$. $\Delta \equiv g\mu_B H_{\text{eff}}/k_B$ becomes

$$\Delta = (g\mu_B/k_B) \sqrt{A(x)H_{\text{ext}}^2 + H_{\text{int}}^2(x)}, \quad (4)$$

where $A(x) = 1 - 2\beta m H_{\text{int}}(x)/3$. In the limit $\beta m H_{\text{ext}} \gg 1$, $L(\beta m H_{\text{ext}}) = 1$ and $\langle \mathbf{H}_{\text{eff}}^2 \rangle = (H_{\text{ext}} - H_{\text{int}}(x))^2$. Hence,

$$\Delta = (g\mu_B/k_B) (H_{\text{ext}} - H_{\text{int}}(x)). \quad (5)$$

We fitted the $\Delta(x)$ vs H_{ext} data of Figs. 3 and 4 with Eqs. 4 and 5, respectively, with $A(x)$ and $H_{\text{int}}(x)$ as fitting parameters. Notice the excellent fits obtained especially for the non-linear $\Delta(x)$ vs H_{ext} data of Fig. 3. When the externally applied magnetic field is large enough, it aligns the net magnetic moment in its direction, hence, Δ becomes proportional to the resultant magnetic field [Eq. (5)]. In this high field region where the superconducting contribution of the $0.05 \leq x \leq 0.5$ samples or the antiferromagnetic contribution of the $0.7 \leq x \leq 0.9$ samples is suppressed below 0.5 K, Δ increases linearly with H_{ext} with a doping-independent slope [see Fig. 4]. Least-square linear fits of Δ vs H_{ext} in this higher field region give $g\mu_B/k_B \approx 1.4$, which corresponds to $g = 2$ as expected for the ground state $^8S_{7/2}$ of Eu.

CONCLUSIONS

We analyzed the low-temperature specific heat data in order to investigate the interaction between magnetism and superconductivity and reveal the effect of magnetic field on the nature of the superconducting and antiferromagnetic orders in the $\text{Pr}_{1-x}\text{Eu}_x\text{Pt}_4\text{Ge}_{12}$ filled skutterudite system. Our data show the presence of short range AFM correlations between Eu ions under the superconducting region for $x \leq 0.50$. These short range AFM correlations produce a local internal magnetic field, which, along with the applied magnetic field, lifts the eight-fold degeneracy of the Eu ground state and gives rise to a Schottky anomaly in heat capacity that shifts to higher temperature with increasing H_{ext} . In the higher Eu substituted samples, i.e. in the doping range $0.7 \leq x \leq 0.9$,

the samples display a peak due to AFM. The Néel temperature is suppressed with increasing H_{ext} . With further increasing applied field, the heat capacity reveals a Schottky anomaly that shifts towards higher temperature with further increasing magnetic field. The low temperature heat capacity data can be fitted with the sum of a superconducting/normal state term and a Schottky term. At low values of H_{ext} , the internal and external magnetic fields are comparable, hence the Schottky gap shows a super-linear dependence on H_{ext} . High applied magnetic field aligns the internal moment in its direction, hence the Schottky anomaly increases linearly with H_{ext} with a doping-independent slope, as normally expected.

ACKNOWLEDGMENTS

This work was supported by the National Science Foundation grants DMR-1505826 and DMR-1506547 at KSU and by the US Department of Energy, Office of Basic Energy Sciences, Division of Materials Sciences and Engineering, under Grant No. DE-FG02-04ER46105 at UCSD. The work of M. D. and P. S. was financially supported in part by the U.S. Department of Energy, Office of Basic Energy Sciences under Award No. DE-SC0016481.

-
- [1] A. Maisuradze, M. Nicklas, R. Gumeniuk, C. Baines, W. Schnelle, H. Rosner, A. Leithe-Jasper, Y. Grin, and R. Khasanov, *Phys. Rev. Lett.* **103**, 147002 (2009).
 - [2] L. S. Chandra, M. Chattopadhyay, and S. Roy, *Philosophical Magazine* **92**, 3866 (2012).
 - [3] J. Zhang, Y. Chen, L. Jiao, R. Gumeniuk, M. Nicklas, Y. Chen, L. Yang, B. Fu, W. Schnelle, H. Rosner, et al., *Physical Review B* **87**, 064502 (2013).
 - [4] Y. Nakamura, H. Okazaki, R. Yoshida, T. Wakita, H. Takeya, K. Hirata, M. Hirai, Y. Muraoka, and T. Yokoya, *Physical Review B* **86**, 014521 (2012).
 - [5] Y. P. Singh, R. B. Adhikari, S. Zhang, K. Huang, D. Yazici, I. Jeon, M. B. Maple, M. Dzero, and C. C. Almasan, *Phys. Rev. B* **94**, 144502 (2016).
 - [6] A. Maisuradze, W. Schnelle, R. Khasanov, R. Gumeniuk, M. Nicklas, H. Rosner, A. Leithe-Jasper, Y. Grin, A. Amato, and P. Thalmeier, *Physical Review B* **82**, 024524 (2010).
 - [7] Y. Aoki, A. Tsuchiya, T. Kanayama, S. Saha, H. Sugawara, H. Sato, W. Higemoto, A. Koda, K. Ohishi, K. Nishiyama, et al., *Physical review letters* **91**, 067003 (2003).
 - [8] E. Bauer, A. Ślebarnski, N. Frederick, W. Yuhasz, M. Maple, D. Cao, F. Bridges, G. Giester, and P. Rogl, *Journal of Physics: Condensed Matter* **16**, 5095 (2004).
 - [9] C. Sekine, K. Akahira, K. Ito, and T. Yagi, *Journal of the Physical Society of Japan* **78**, 093707 (2009).
 - [10] V. V. Krishnamurthy, J. C. Lang, D. Haskel, D. J. Keavney, G. Srajer, J. L. Robertson, B. C. Sales, D. G.

- Mandrus, D. J. Singh, and D. I. Bilc, Phys. Rev. Lett. **98**, 126403 (2007).
- [11] W. Schnelle, A. Leithe-Jasper, H. Rosner, R. Cardoso-Gil, R. Gumeniuk, D. Trots, J. Mydosh, and Y. Grin, Physical Review B **77**, 094421 (2008).
- [12] M. Nicklas, R. Gumeniuk, W. Schnelle, H. Rosner, A. Leithe-Jasper, F. Steglich, and Y. Grin, Journal of Physics: Conference Series **273**, 012118 (2011).
- [13] A. Grytsiv, X.-Q. Chen, N. Melnychenko-Koblyuk, P. Rogl, E. Bauer, G. Hilscher, H. Kaldarar, H. Michor, E. Royanian, R. Podloucky, et al., Journal of the Physical Society of Japan **77**, 121 (2008).
- [14] N. R. Leigh and D. P. Hampshire, Phys. Rev. B **68**, 174508 (2003).
- [15] U. Köhler, R. Demchyna, S. Paschen, U. Schwarz, and F. Steglich, Physica B: Condensed Matter **378**, 263 (2006).
- [16] D. Naugle, K. Rathnayaka, V. Krasovitsky, B. Belevtsev, M. Anatska, G. Agnolet, and I. Felner, Journal of applied physics **99**, 08M501 (2006).
- [17] E. D. Bauer, N. A. Frederick, P.-C. Ho, V. S. Zapf, and M. B. Maple, Physical Review B **65**, 100506 (2002).
- [18] N. A. Frederick, T. A. Sayles, and M. B. Maple, Phys. Rev. B **71**, 064508 (2005).
- [19] N. Takeda and M. Ishikawa, Journal of the Physical Society of Japan **69**, 868 (2000).
- [20] The response of Pr-based skutterudite superconductors to an external magnetic field strongly depends on the specific structure of Pr^{3+} crystalline electric field (CEF). For example, the analysis of the CEF for $\text{PrRu}_4\text{Sb}_{12}$ shows that its ground state is Γ_1 singlet and its first-excited Γ_4 triplet is 73 K above [19]. However, the first excited CEF level of $\text{PrPt}_4\text{Ge}_{12}$ is at 131 K [31] above its ground state singlet. This latter CEF scheme has been confirmed by inelastic neutron scattering [32]. Thus, in these two SC compounds (i) the ground state is actually a non-magnetic singlet and (ii) the CEF splitting is much larger than in $\text{PrOs}_4\text{Sb}_{12}$ [17], which is the only heavy-fermion.
- [21] Y. Aoki, T. Namiki, S. Ohsaki, S. R. Saha, H. Sugawara, and H. Sato, Journal of the Physical Society of Japan **71**, 2098 (2002).
- [22] R. B. Adhikari, D. L. Kunwar, I. Jeon, M. B. Maple, M. Dzero, and C. C. Almasan, Phys. Rev. B **98**, 064506 (2018).
- [23] I. Jeon, K. Huang, D. Yazici, N. Kanchanavatee, B. D. White, P.-C. Ho, S. Jang, N. Pouse, and M. B. Maple, Phys. Rev. B **93**, 104507 (2016).
- [24] B. H. Toby, Journal of Applied Crystallography **34**, 210 (2001).
- [25] I. Jeon, S. Ran, A. J. Breindel, P.-C. Ho, R. B. Adhikari, C. C. Almasan, B. Luong, and M. B. Maple, Phys. Rev. B **95**, 134517 (2017).
- [26] E. S. R. Gopal, *Magnetic Contribution to Specific Heats* (Springer US, Boston, MA, 1966), pp. 84–111, ISBN 978-1-4684-9081-7.
- [27] L. Liu, S. Bi, B. Peng, and Y. Li, Journal of Applied Physics **117**, 17E117 (2015).
- [28] Z. Guguchia, S. Bosma, S. Weyeneth, A. Shengelaya, R. Puzniak, Z. Bukowski, J. Karpinski, and H. Keller, Phys. Rev. B **84**, 144506 (2011).
- [29] Anupam, P. L. Paulose, S. Ramakrishnan, and Z. Hos-sain, Journal of Physics: Condensed Matter **23**, 455702 (2011).
- [30] Z. Ren, Q. Tao, S. Jiang, C. Feng, C. Wang, J. Dai, G. Cao, and Z. Xu, Phys. Rev. Lett. **102**, 137002 (2009).
- [31] R. Gumeniuk, W. Schnelle, H. Rosner, M. Nicklas, A. Leithe-Jasper, and Y. Grin, Physical review letters **100**, 017002 (2008).
- [32] E. A. Goremychkin, D. T. Adroja, A. D. Hillier, and R. Osborne, unpublished (2009).